Hierarchical Membranes

DOI: 10.1002/anie.201005222

Ordered Hierarchical Porous Platinum Membranes with Tailored Mesostructures**

Xinyi Zhang, Wei Lu, Jiyan Dai, Laure Bourgeois, Na Hao, Huanting Wang, Dongyuan Zhao, and Paul A. Webley**

Porous metallic materials are of significant interest in a wide variety of applications, including catalysis, energy storage, sensing, and separation to biotechnology.[1] It is widely acknowledged that templating techniques have great advantages in fabricating ordered porous materials. With these techniques, many porous metals have been fabricated by using block copolymer, colloidal crystals, polymer microspheres, and porous anodic alumina.[2] Ordered metal nanostructures with hierarchical porosity, namely macropores in combination with mesopores, are of particular interest because macropores allow access to large guest molecules, and an efficent mass transport through the porous structures is enabled whilst mesopores can enhance the active surface area.[3] For example, in fuel cell electrodes, a bimodal pore size distribution in porous metallic materials composed of macroporous channels with mesopore walls is highly desirable to achieve fast mass transfer and high electroactivity.

Self-assembly and formation of mesoporous metals within the void space of template are a key step toward metal nanostructures with hierarchical porosity. Since the pioneering work by Attard et al.,[4] various ordered mesoporous metals have been prepared from lyotropic liquid-crystal (LLC) phases composed of self-assembled nonionic surfactants, such as octaethylene glycol monohexadecyl ether ($C_{16}EO_8$).[5] In the previous work, surfactants, water, and metal compounds were mixed vigorously and subjected to several heating/cooling cycles to obtain a homogeneous LLC phase. Mesoporous metals were synthesized from the highly viscous ternary mixtures at high concentrations of surfactant (about 38 wt% or above) and low temperatures (ca. 25 °C).[4,6a] With respect to the LLC templating method for the production of ordered hierarchical porous metals, there are two challenging issues: 1) how to uniformly and controllably prepare ordered mesoporous metals in the void space of templates, as the viscosity of the LLC mixture is very high; and 2) how to control LLC mesophases so that porous metals with designed and controlled mesostructures can be generated in the void space of templates. In nanoscopic systems, the confinement breaks the symmetry of the bulk phase and the resulting structure much depends on elastic forces, surface coupling, and curvature effects.[7] Although some experimental efforts have been made,[8] the synthesis of ordered porous metals with controlled geometry and mesostructure still remains an important challenge.

We have developed a novel two-step method to prepare metals with designed mesostructure and geometry. Herein we report the fabrication of ordered hierarchical porous platinum membranes utilizing $C_{16}EO_8$ as a LLC former and reverse porous PMMA cast from porous anodic alumina (PAA) as a hard template. The obtained Pt membranes have ordered mesopores and tunable large macropore channels, and continuous frameworks that are very similar to those of PAA templates. Moreover, we demonstrate that the mesostructure in the Pt membranes can be tailored by controlling the concentration of $C_{16}EO_8$ solution.

Figure 1 shows scanning electron microscopy (SEM) images of the porous Pt membrane with about 68 nm pore diameter prepared by using a 55 wt% $C_{16}EO_8$ solution. Figure 1a shows the top surface view of the Pt membrane; it can be clearly seen that the Pt membranes retain the

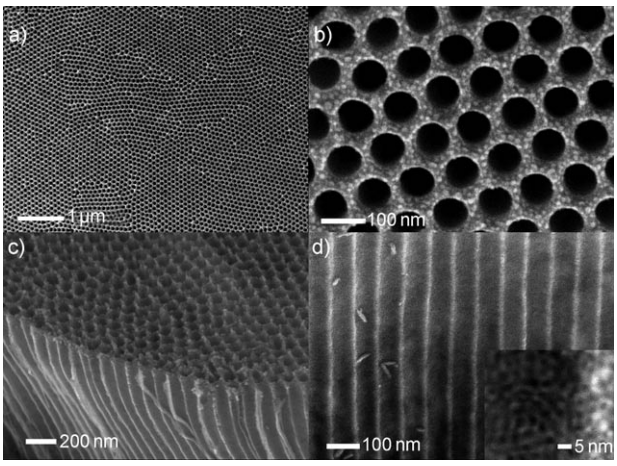

Figure 1. SEM images of ordered hierarchical porous Pt membranes. a) Surface view; b) enlarged surface view; c) oblique view; d) cross-sectional view. Inset: a high-resolution image of the channel wall.

[*] Dr. X. Y. Zhang, N. Hao, Prof. Dr. H. T. Wang, Prof. Dr. D. Y. Zhao, Prof. Dr. P. A. Webley
Department of Chemical Engineering, Monash University
Clayton, VIC3800 (Australia)
Fax: (+61) 3-9905-5686
E-mail: xinyi.zhang@monash.edu.au
paul.webley@monash.edu.au
Dr. W. Lu, Prof. Dr. J. Y. Dai
Department of Applied Physics
The Hong Kong Polytechnic University (China)
Dr. L. Bourgeois
Monash Centre for Electron Microscopy
Monash University (Australia)

[**] This work was supported by the Australian Research Council and Monash University. X.Z. thanks the Australian Research Council for the ARF Fellowship.

Supporting information for this article is available on the WWW under http://dx.doi.org/10.1002/anie.201005222.

dimension, morphology, and structure of the alumina templates, exhibiting a uniform pore size and highly ordered pore arrangement over a large area. The enlarged surface image in Figure 1b shows that the nanopores are hexagonally arranged in a high regularity. The wall thickness and the interpore distance of the porous Pt membranes are about 37 and 105 nm, respectively. The oblique view of the Pt membrane in Figure 1c shows the bottom surface and parallel cylindrical channels with a length of about 1 μm. The cross-sectional view of the Pt membrane is given in Figure 1d. The high-resolution SEM images (inset in Figure 1d; see also Figure S1 in the Supporting Information) show that the Pt membranes consist of uniform mesopores templated from the nonionic surfactant LLC.

The porous Pt membranes were further investigated by transmission electron microscopy (TEM). The highly ordered macroporous structure of the Pt membrane is given in Figure 2a,b. The inset in Figure 2a shows the corresponding

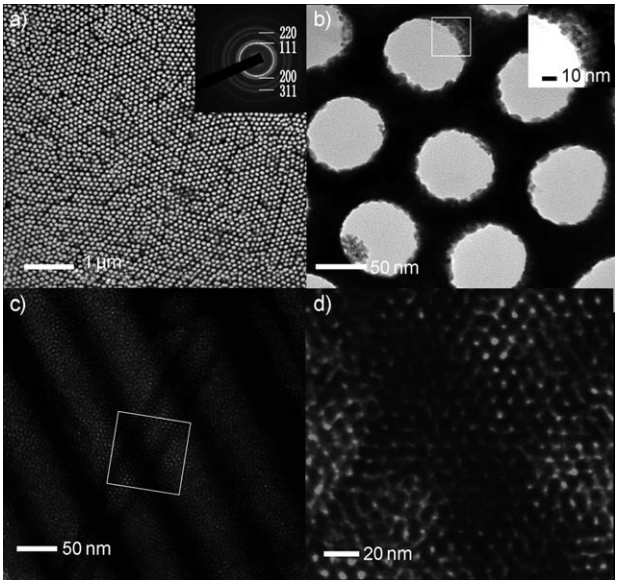

Figure 2. TEM images of highly ordered hierarchical porous Pt membranes. a,b) Plane views with different magnifications and the corresponding electron-diffraction pattern (inset in (a)); c) cross-sectional view; d) enlarged cross-sectional view from area marked in (c), showing an ordered mesostructure.

electron diffraction (ED) pattern. The continuous strong rings can be indexed as the face-centered cubic (FCC) Pt structure, which is in accordance with X-ray diffraction (XRD) analysis (Figure S2 in the Supporting Information). Mesochannels are visible at the edge of the pores (inset, Figure 2b) and more mesochannels can be observed by tilting the sample (Figure S3 in the Supporting Information). Figure 2c shows the TEM image of the cross-sectional view of the porous Pt membrane. It is apparent that the pore wall domains appear darker than the void parts in the image. A high-magnification TEM image of the region indicated in Figure 2c is given as Figure 2d, where hexagonally organized mesopores with pore size of 2–3 nm can clearly be observed (see also Figure S4 in the Supporting Information). The high-

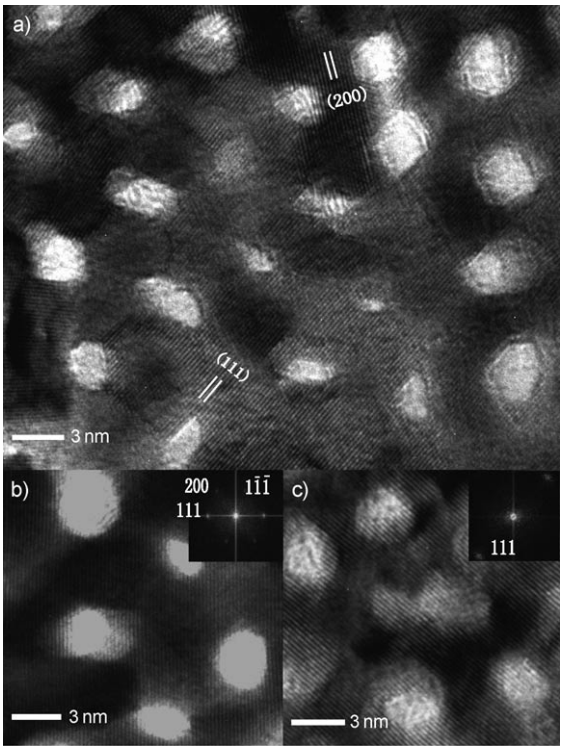

Figure 3. HRTEM images of a) the mesoporous Pt channel walls with a continuous network structure, and b,c) the single-crystalline Pt regions and the corresponding Fourier transform patterns (insets).

resolution TEM (HRTEM) image of the mesopore wall in the porous Pt membrane is given as Figure 3a. The well-resolved lattice spacings of 0.22 and 0.20 nm correspond to the Pt {111} and {200} atomic planes, respectively. The interpore distance is about (6 ± 1) nm, which is consistent with the lattice parameter (ca. 6 nm) of the hexagonal mesophase of $C_{16}EO_8$ LLC.[4b] The deformation of the mesopores can be observed, which is probably caused by the imperfect alignment of the LLC mesophase on the curved surface of PMMA nanorods (Figure S5 in the Supporting Information). The mesoporous Pt membranes are polycrystalline, but single crystalline domains with size up to hundreds of nanometers can be unmistakably observed in spite of the existence of mesopores. Figure 3b,c shows the HRTEM images of the single crystalline regions. This is further confirmed by the Fourier transform patterns (inset, Figure 3b,c). The surface of the single-crystalline regions can be identified as the {110} planes of FCC Pt structure. This is advantageous for applications in fuel cell, as the activity for oxygen reduction on {110} of Pt is known to be the highest among low-index crystallographic planes in nonadsorbing electrolyte.[9]

Fabrication of materials with designed and tunable mesostructures is much in demand for practical applications because the material properties largely depend on the structures.[10] According to the phase diagram, several other mesophases, including a lamellar phase, can be formed in the binary $C_{16}EO_8$/water system under different conditions.[6] Therefore, different mesostructures can be designed and fabricated by LLC templating. Figure 4a,b show plane-view SEM images of the Pt membrane replicated from PAA

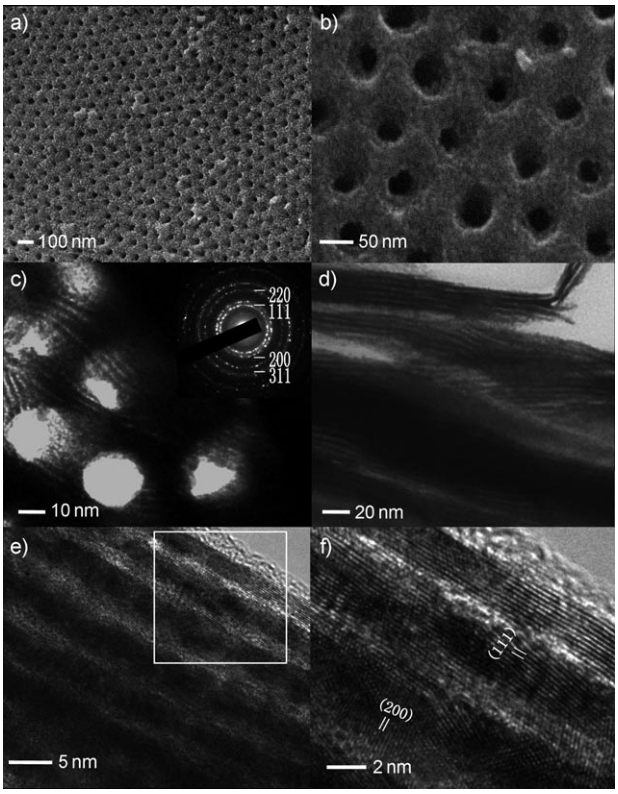

Figure 4. Hierarchical porous Pt membrane with lamellar structure: a,b) Plane-view SEM images at different magnifications, c) plane-view TEM image and the corresponding electron diffraction pattern. d,e) Cross-sectional TEM images at different magnifications; f) HRTEM image.

template, with pore diameter of about 45 nm, by using a 70 wt% $C_{16}EO_8$ solution. The Pt membrane replicates the ordered nanoporous structure of the PAA template; the decrease in size and deformation of the nanopores in the Pt membrane can also be observed. Layered mesophase can be unmistakably identified from the TEM images of the porous Pt membrane. It can be seen that the nanopores are surrounded by both twisted continuous and disconnected mesophase layers (Figure 4c). The thickness of the layers and interchannel distance of the lamellar mesostructure are determined to be 2–3 and 4 nm, respectively. Stacked multilayers with ordered mesoporous channels of several hundreds of nanometers in length can be distinctly observed from the cross-sectional views, and the mesochannels are predominantly oriented parallel to the cavity walls of the Pt membrane (Figure 4d,e; see also Figure S6 in the Supporting Information). The corresponding ED pattern (inset in Figure 4c) and XRD pattern (Figure S2 in the Supporting Information) show that the Pt membrane has a FCC structure. These results clearly demonstrate the formation of the hierarchical porous Pt membrane with a lamellar mesostructure in which the stacked layers align perpendicular to the surface of Pt membrane. The plane-view TEM observations reveal that the mesophases are forced to split into twisted layers when they meet with PMMA nanorods. This should result in high stress in LLC. Besides, the LLC mesophase is compressed during the Pt deposition between the lamellar layers, which also increases the stress in the system. The LLC mesophase could release the stress through expansion after the removal of the PMMA template, which leads to the decrease and deformation of the nanopores in the porous Pt membrane. This proposition is supported by the fact that the deformation and decrease of the nanopores surrounded by the disconnected layers are smaller than those surrounded by the twisted continous layers. Figure 4f shows a HRTEM image of the region indicated in Figure 4e, where clear (111) and (200) lattice fringes with respective spacings of 0.22 and 0.20 nm are visible. It is worth noting that the interchannel distance of the lamellar mesophase is much smaller than the interpore distance of the hexagonal mesophase, revealing a higher packing density of the lamellar mesophase in comparison with the hexagonal mesophase.

Figure 5 illustrates the preparation process of ordered hierarchical porous Pt membranes. The formation of LLC phase within the nanoscale void space of PMMA template is the first step toward ordered mesoporous metals. The phase

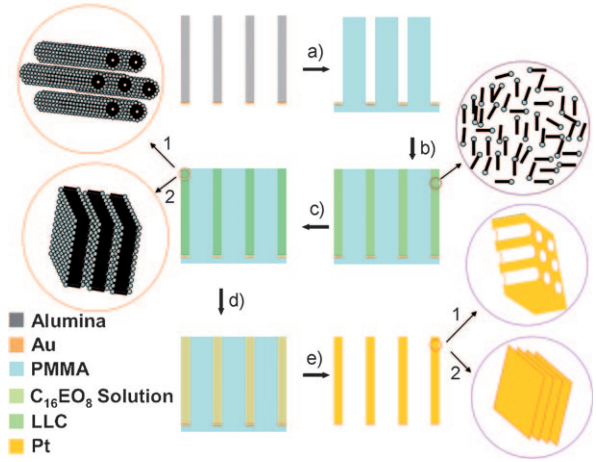

Figure 5. Illustration of the preparation of hierarchical porous Pt membranes. a) Preparation of the negative poly(methyl methacrylate) (PMMA) template from porous anodic alumina; b) injection of $C_{16}EO_8$ solution; c) formation of LLC within the PMMA template; d) electroless deposition of Pt; e) removal of the PMMA. $C_{16}EO_8$ concentration: 1) 55 wt%, 2) 70 wt%.

transformation from micellar solution into LLC occurs when the temperature is below the melting point of the LLC. The building elements of LLCs are formed by the aggregation of amphilic $C_{16}EO_8$ molecules into large anisotropic micelles, where hydrophlic EO head groups at the interface shield hydrophobic alkyl chains from contact with water. In our experiments, LLC phases are formed from the homogeneous binary $C_{16}EO_8/H_2O$ system. The micellar solutions have high mobility and can be uniformly loaded into the void space of PMMA template, and the subsequent cooling process allows the formation of ordered and stable LLC phases in the nanoscale void geometry of the PMMA template. The mesostructure of LLC phases can be directly designed according to the binary $C_{16}EO_8/H_2O$ phase diagram.[6] When the concentration of $C_{16}EO_8$ is 55 wt%, rod micelles are

formed by the aggregation of $C_{16}EO_8$ molecules, which then close-pack into hexagonal arrays during the cooling process. Upon increasing the concentration of $C_{16}EO_8$ to 70 wt%, the volume faction of micelles is above the close-packing limit of rod micelles, lamellar mesophases with water sandwiched structure between the layers occur. Previously, it has been suggested that the generation of mesoporous metals is through the interaction between metal ions and the EO headgroups of the surfactant.[4b,6a] Our experiments reveal that the templating mechanism of LLC phases can be exactly the same as that of a hard template. During the Pt deposition, the LLC phases are intact and act as structure-directing media in the generation of mesoporous metal and determines the order and orientation of mesostructures in the Pt membranes. The Pt deposition starts at the bottom of the cavity of the PMMA template because plating only takes place in the presence of a catalyst. The deposition proceeds through the diffusion of Pt ions into the mesochannels of LLC phases and the mesostructured metal gradually fills the cavity of the PMMA template.

In the LLC-loaded PMMA template, the deposition rate of Pt is very slow owing to the low diffusion rate of Pt ions in the nanoscale voids. In this situation, the oriented (or epitaxial) growth of existing grains could be thermodynamically favorable in comparison with the nucleation of new grains. It has been well-documented that oriented growth in nanochannels of PAA templates can result in single crystalline nanowires.[11] We believe that the confinement of the narrow nanovoids in PMMA template and the low growth rate at low temperatures should be mainly responsible for the formation of the single crystalline domains in the Pt membranes. When the deposition reaches the LLC rods, these ultrathin LLC rods could be embedded into such domains without changing the structural continuity of the matrix, resulting in the single-crystalline mesoporous regions in the Pt membranes.

In summary, ordered hierarchical porous platinum membranes have been fabricated for the first time by a two-step method that utilizes the nonionic surfactant $C_{16}EO_8$ LLC as a mesostructural template and reverse porous PMMA cast from porous anodic alumina as a macroscopic template. One important advantage of our new method is that it can be used to synthesize ordered mesoporous metals in a very confined void space with designed composition, structure, and geometry. We have also successfully synthesized platinum nanowires with ordered hexagonal and lamellar mesostructures, respectively (Figure S7 in the Supporting Information). Furthermore, this method is simple and can be extended to other metals, alloys, or oxides. Such hierarchically ordered porous metal membranes may open up a new opportunity for numerous applications, such as flow-through electrodes in sensors and fuel cells.

Experimental Section

A two-step method was developed to prepare ordered metal mesostructures with a designed geometry. First, a homogeneous binary oligomeric nonionic surfactant solution was prepared and loaded into a template at a high temperature, and then the template was cooled down to allow the formation of an ordered and stable LLC in the void space of the template. Second, the LLC phases act as mesostructural templates, and metals are fabricated in the void space of the LLC-loaded template by electroless- or electro-deposition. Ordered hierarchical porous Pt membranes were fabricated as follows: The reverse porous poly(methyl methacrylate) (PMMA) templates were prepared from porous anodic alumina by a replication method.[2e] The polymerization of methyl methacrylate was carried out at 85 °C for 10 h. The binary mixtures of non-ionic surfactant $C_{16}EO_8$/water were stirred and heated to form a uniform micellar solution. $C_{16}EO_8$ (0.05–0.15 g, 55 wt%) and $C_{16}EO_8$ (0.065–0.2 g, 70 wt%) solutions were used for the formation of hexagonal LC and lamellar LC phases, respectively. The $C_{16}EO_8$ solution was dropped onto a PMMA template and the sample was sealed and maintained under constant temperature (65 °C for hexagonal LC phases and 80 °C for lamellar LC phases) for 12 h. The template was then cooled down to 28 °C. A saturated K_2PtCl_4 solution (ca. 2 g K_2PtCl_4 in 10 mL aqueous solution) was used as the Pt plating solution. The LLC-loaded PMMA template was immersed into 0.1–1 mL Pt plating solution, and electroless Pt deposition was carried out at 28 °C for 10 h. Finally, porous Pt membranes were obtained by dissolving the PMMA with acetone. The morphology and microstructure of the Pt membranes was investigated using a scanning electron microscope (SEM, JEOL JSM-7100) and transmission electron microscopes (TEM, JEOL-2011 and JEOL-2100F).

Received: August 20, 2010
Published online: November 29, 2010

Keywords: lyotropic liquid crystals · mesostructures · platinum · porous materials · template synthesis

[1] a) D. Walsh, L. Arcelli, T. Ikoma, J. Tanaka, S. Mann, *Nat. Mater.* **2003**, *2*, 386–390; b) J. Erlebacher, M. J. Aziz, A. Karme, N. Dimitrov, K. Sieradzki, *Nature* **2001**, *410*, 450–453; c) O. D. Velev, E. C. Kaler, *Adv. Mater.* **2000**, *12*, 531–534.

[2] a) S. C. Warren, L. C. Messina, L. S. Slaughter, M. Kamperman, Q. Zhou, S. M. Grunner, F. J. Dislvo, U. Wiesner, *Science* **2008**, *320*, 1748–1752; b) Z. Chen, P. Zhan, Z. L. Wang, J. H. Zhang, N. B. Ming, C. T. Chan, P. Sheng, *Adv. Mater.* **2004**, *16*, 417–422; c) P. N. Bartlett, J. J. Baumberg, P. R. Birkin, M. A. Ghanem, M. C. Netti, *Chem. Mater.* **2002**, *14*, 2199–2208; d) P. Jiang, J. Cizeron, J. F. Colvin, *J. Am. Chem. Soc.* **1999**, *121*, 7957–7958; e) H. Masuda, K. Fukuda, *Science* **1995**, *268*, 1466–1468.

[3] L. H. Lu, A. Eychmller, *Acc. Chem. Res.* **2008**, *41*, 244–253.

[4] a) G. S. Attard, P. N. Bartlett, N. R. B. Coleman, J. M. Elliott, J. R. Owen, J. H. Wang, *Science* **1997**, *278*, 838–840; b) G. S. Attard, C. G. Göltner, J. M. Corker, S. Henke, R. H. Templer, *Angew. Chem.* **1997**, *109*, 1372–1374; *Angew. Chem. Int. Ed. Engl.* **1997**, *36*, 1315–1317.

[5] a) Y. Yamauchi, A. Takai, M. Komatsu, M. Sawada, T. Ohsuna, K. Kuroda, *Chem. Mater.* **2008**, *20*, 1004–1011; b) P. V. Braun, P. Osenar, M. Twardowski, G. N. Tew, S. I. Stupp, *Adv. Funct. Mater.* **2005**, *15*, 1745–1750; c) T. Kijima, T. Yoshimura, M. Uota, T. Ikeda, D. Fujikawa, S. Mouri, S. Uoyama, *Angew. Chem.* **2004**, *116*, 230–234; *Angew. Chem. Int. Ed.* **2004**, *43*, 228–232; d) P. A. Nelson, J. M. Elliott, G. S. Attard, J. R. Owen, *Chem. Mater.* **2002**, *14*, 524–529; e) A. H. Whitehead, J. M. Elliott, J. R. Owen, G. S. Attard, *Chem. Commun.* **1999**, 331–332.

[6] a) G. S. Attard, P. N. Bartlett, N. R. B. Coleman, J. M. Elliott, J. R. Owen, *Langmuir* **1998**, *14*, 7340–7342; b) D. J. Mitchell, G. J. Tiddy, L. Waring, T. Bostock, M. P. McDonald, *J. Chem. Soc. Faraday Trans.* **1983**, *79*, 975–1000.

[7] a) J. Z. Y. Chen; D. E. Sullivan, X. Q. Yuan, *Macromolecules* **2007**, *40*, 1187–1195; D. E. Sullivan, X. Q. Yuan, *Macromole-*

cules **2007**, *40*, 1187 – 1195; b) S. G. Cloutier, J. N. Eakin, R. S. Guico, M. E. Sousa, G. P. Crawford, J. M. Xu, *Phys. Rev. E* **2006**, *73*, 0517039; c) B. Jérôme, *Rep. Prog. Phys.* **1991**, *54*, 391 – 451.

[8] a) A. Takai, T. Saida, W. Sugimoto, L. Wang, Y. Yamauchi, K. Kuroda, *Chem. Mater.* **2009**, *21*, 3414 – 3423; b) Y. Yamauchi, A. Takai, T. Nagaura, S. Inoue, K. Kuroda, *J. Am. Chem. Soc.* **2008**, *130*, 5426 – 5427; c) L. H. Lu, R. Capek, A. Kornowski, N. Gaponik, A. Eychmüller, *Angew. Chem.* **2005**, *117*, 6151 – 6155; *Angew. Chem. Int. Ed.* **2005**, *44*, 5997 – 6001; d) Y. Yamauchi, T. Momma, H. Kitoh, T. Osaka, K. Kuroda, *Electrochem. Commun.* **2005**, *7*, 1364 – 1370; e) Y. Y. Wu, T. Livneh, Y. X. Zhang, G. S. Cheng, J. F. Wang, J. Tang, M. Moskovits, G. D. Stucky, *Nano Lett.* **2004**, *4*, 2337 – 2342; f) Y. Y. Wu, G. S. Cheng, K. Katsov, S. W. Sides, J. Wang, J. Tang, G. H. Fredrickson, M. Moskovits, G. D. Stucky, *Nat. Mater.* **2004**, *3*, 816 – 822.

[9] N. Markovic, H. Gasteiger, P. N. Ross, *J. Electrochem. Soc.* **1997**, *144*, 1591 – 1597.

[10] a) A. Takai, Y. Yamauchi, K. Kuroda, *J. Am. Chem. Soc.* **2010**, *132*, 208 – 214; b) J. Y. Jiang, O. V. Lima, Y. Pei, X. C. Zeng, L. Tan, E. Forsythe, *J. Am. Chem. Soc.* **2009**, *131*, 900 – 901; c) B. Platschek, N. Petkov, T. Bein, *Angew. Chem.* **2006**, *118*, 1152 – 1156; *Angew. Chem. Int. Ed.* **2006**, *45*, 1134 – 1138; d) A. Yamaguchi, F. Uejo, T. Yoda, T. Uchida, Y. Tanamur, T. Yamashita, N. Teramae, *Nat. Mater.* **2004**, *3*, 337 – 341.

[11] a) W. Wang, X. L. Lu, T. Zhang, G. Q. Zhang, W. J. Jiang, X. G. Li, *J. Am. Chem. Soc.* **2007**, *129*, 6702 – 6703; b) Z. Miao, D. S. Xu, J. H. Ouyang, G. L. Guo, X. S. Zhao, Y. Q. Tang, *Nano Lett.* **2002**, *2*, 717 – 720.

